

Doubling of the orbital magnetic moment in nanoscale Fe clusters

K. W. Edmonds, C. Binns, S. H. Baker, S. C. Thornton, and C. Norris

Department of Physics and Astronomy, University of Leicester, Leicester LE1 7RH, United Kingdom

J. B. Goedkoop, M. Finazzi, and N. B. Brookes

European Synchrotron Radiation Facility, F-38043 Grenoble Cedex, France

(Received 21 December 1998)

Magnetic circular dichroism has been used to study the orbital and spin moments in supported nanoscale Fe clusters deposited *in situ* from a gas aggregation source onto highly oriented pyrolytic graphite in ultrahigh vacuum. Mass-filtered (2.4 nm, 610 atoms) and unfiltered (1–5 nm, 40–5000 atoms) clusters at low coverage have an orbital magnetic moment about twice that of bulk Fe. With increasing coverage the orbital moment of the unfiltered clusters converges to the bulk value. There is no detectable change in the spin moment as a function of coverage. Mass-filtered clusters show an increase in the magnetic dipole moment which we ascribe to distortion resulting from their higher impact energy. An increasing magnetic remanence with coverage is found. [S0163-1829(99)02225-0]

Nanoscale clusters in the size range 1–5 nm (40–5000 atoms) mark the boundary between molecular and solid state systems and have properties distinct from both. The recent surge of interest in them is due to their novel behavior and a growing awareness of their enormous potential in the creation of new materials by deposition from intense mass-selected cluster beams.¹ This can be done in coincidence with a molecular beam of another material so that the clusters form a separated three-dimensional assembly within a matrix. In films produced this way, there is independent control of the size, volume filling fraction, and even the shape (by adjusting the impact velocity) of the clusters allowing a great deal of flexibility in the formation of “designer” materials.

This is especially true of magnetic clusters since magnetism is highly sensitive to the particle size due to several effects. These include the increase in the valence band energy level spacing to a value significant relative to the Zeeman energy $\mu_B H$,² the perturbation of the many-body screening response of the valence electron gas,³ and the reduction in the average atomic coordination. The enhanced proportion of low coordinated atoms at the surface (or interface), which varies from 15 to 75% in the size range considered here, causes a narrowing of the valence *d* band and an increase in the density of states at the Fermi level which increases the spin magnetic moment (m_s) towards the high-spin atomic limit. This has been identified as the cause of the observed increase of the magnetic moment in free Fe, Co, and Ni clusters^{4–7} and the discovery of 4*d* magnetism in Rh particles.⁸ In addition, an enhanced orbital moment (m_l) is expected due to spin-orbit coupling and the reduced symmetry at the surface which leads to a less effective quenching of the orbital moments by the crystal field. An orbital moment of up to four times the bulk value, depending on the bond length, has been predicted for Fe₄ clusters in a rhombohedral arrangement.⁹

The total magnetic moment in free Fe, Co, and Ni clusters was determined as a function of size by measuring their deflection in a Stern-Gerlach field.^{4–7} For large clusters, con-

taining more than about 500 atoms, the bulk value was observed but in all three metals the moment was found to increase with decreasing size and was up to 36% higher than the bulk value in the smallest clusters (20 atoms). There are few results for supported clusters but magnetic moments 30% larger than the bulk value have been reported for nanoscale colloidal Co clusters.¹⁰ In contrast, a recent calculation¹¹ has predicted that very small Ni clusters on graphite are nonmagnetic.

We present here *in situ* x-ray magnetic circular dichroism (XMCD) measurements on *exposed* nanoscale clusters supported on a surface in ultrahigh vacuum (UHV) deposited cleanly from a UHV compatible gas aggregation source. An important advantage of studying adsorbed clusters is the accurate control over the temperature and the possibility of cooling to low cryogenic values which is difficult in the case of free clusters. In addition it is possible to accumulate sufficient densities on the surface to study the effect of interaction. On the other hand, they are not subjected to the large stress imposed by a surrounding matrix. We demonstrate a doubling of the orbital magnetic moment in Fe clusters relative to the bulk and the power of XMCD as a highly sensitive *in situ* probe of orbital and spin magnetic moments.

XMCD in $L_{2,3}$ edge absorption has become an important tool in the study of the magnetic properties of transition metals, especially in thin films and surfaces. The technique is element specific and sensitive to films of less than one monolayer thickness. Application of the sum rules^{12,13} allows a quantitative and independent determination of both orbital and spin magnetic moments m_l and m_s . Despite a number of theoretical and experimental problems,^{14,15} experiments have shown that realistic values of m_l and m_s can be obtained with very high sensitivity.^{16,17}

Here we report XMCD measurements of m_l and m_s in exposed Fe clusters supported on highly oriented pyrolytic graphite (HOPG) with sizes in the range 1–5 nm (40–5000 atoms) as a function of their density on the surface. The experiment was conducted on beamline ID 12B of the ESRF, Grenoble on a helical undulator source (Helios-I) producing

intense radiation of selectable helicity with an $85 \pm 5\%$ degree of circular polarization at the Fe L edge.¹⁸ The monochromatic light was obtained with a dragon type monochromator operated at an energy resolution of 0.2 eV. The measurements were made in a 7 T cryomagnet with a base pressure of $< 2 \times 10^{-10}$ mbar.

HOPG surfaces were prepared by cleaving in air and heating to $\sim 250^\circ\text{C}$ in a UHV sample preparation chamber with a base pressure of 1×10^{-10} mbar, before transferring into the magnet. An earlier photoemission study has shown that any measurable contaminants can be removed by this technique.¹⁹ Fe cluster films were deposited on the substrates *in situ* using a portable, UHV-compatible gas-aggregation cluster source, described elsewhere,²⁰ attached to the magnet. The substrate temperature was maintained at 10 K during the film growth and all subsequent measurements. In some depositions, the clusters were size selected using a quadrupole filter, axial with the beam, and capable of filtering masses up to 32 000 amu with a resolving power of up to 100.²⁰ Transmission electron microscopy²⁰ and scanning tunneling microscopy (STM) (Refs. 21 and 22) studies of Fe and Mn particles deposited by this source have shown that the unfiltered beam has an asymmetric log-normal size distribution with the peak at 2.3 nm and a median diameter of 3.1 nm. The cluster density on the surface could be determined by integrating the drain current from a grid placed in the beam during deposition, and from the XAS signal-to-background ratio (edge jump). In the following, using a previous calibration, we have converted the integrated current to the equivalent thickness, in \AA of a continuous Fe film. The random error in the thickness measurement is 1% and the systematic error is 15%. Results are presented for thicknesses in the range 0.25 to 11.3 \AA which for 2.3 nm clusters corresponds to a cluster coverage between approximately 2 and 90% assuming a close-packed layer.

The XAS spectra were obtained by measuring the total sample drain current with the sample normal and applied magnetic field parallel to the photon beam direction, thus minimizing saturation effects.¹⁷ Dichroism measurements were taken by reversing either the field direction \mathbf{H} or the photon spin polarization σ . The data were flux normalized, and scaled to the same edge jump after subtraction of a linear background, so that the measured dichroism is ‘‘per atom.’’²³

Normalized XAS spectra $I(\omega)$ for parallel $I_{\uparrow\uparrow}(\omega)$ and antiparallel $I_{\uparrow\downarrow}(\omega)$, \mathbf{H} and σ taken from a low density (1.1 \AA) cluster film without mass-selection, are shown in Fig. 1(a). No shoulders, characteristic of contamination in the clusters, are visible. Also, even at the lowest coverages studied (0.25 \AA), the spectra are smooth, lacking the detailed structure expected for an atomiclike ground state.²⁴ The branching ratio (ratio of the L_3 intensity to the total $L_3 + L_2$ intensity averaged over both configurations), as well as the total intensity [proportional to the number of valence band holes n_h (Ref. 25)], are constant to within 1 and 5%, respectively, with coverage.

Figure 1(b) shows $L_{2,3}$ XMCD spectra together with their integrals, after normalizing the spectra as described earlier. Data is shown for unfiltered Fe cluster films at the minimum and maximum densities studied and it is clear that the

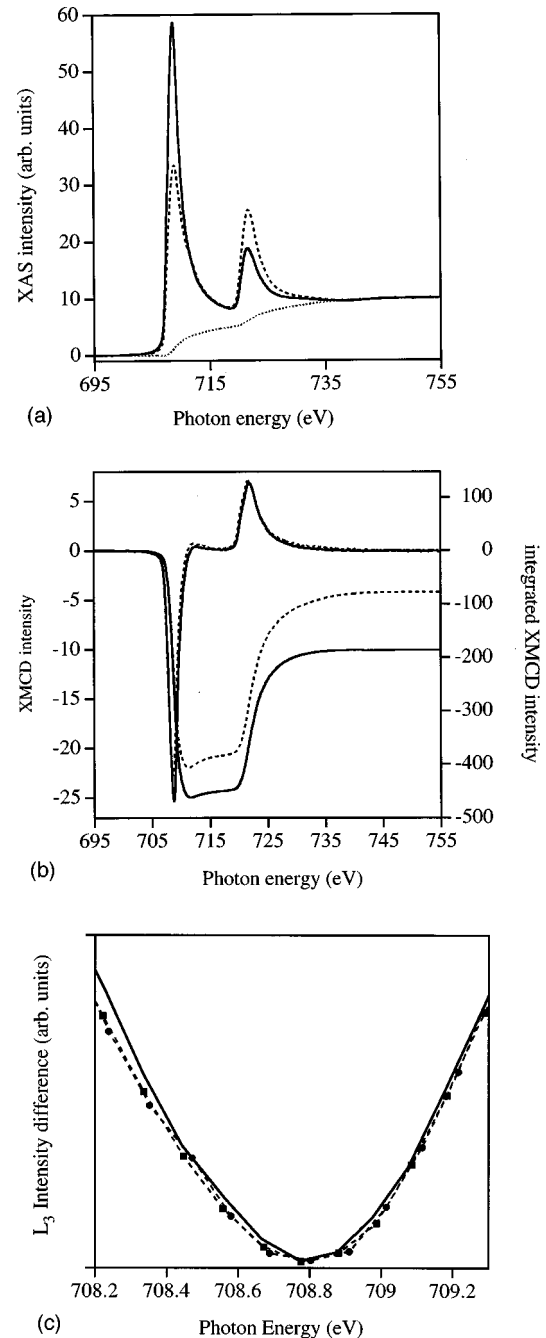


FIG. 1. (a) XAS spectra for \mathbf{M} and σ antiparallel (full line) and parallel (broken line), for a 1.1 \AA thick Fe cluster film. Also shown is the step function used for background subtraction in the spin-averaged spectrum. (b) $L_{3,2}$ XMCD spectrum and integrated XMCD signal, for 1.1 \AA (solid lines) and 11.3 \AA (broken lines) Fe cluster films. (c) L_3 XMCD spectra for a 0.25 \AA mass-selected film (solid line), and for two unfiltered depositions with effective thicknesses of 1.1 \AA (dashed line, squares) and 11.3 \AA (dashed line, circles). To facilitate the comparison the L_3 peak positions have been shifted to the same value.

branching ratio of the L_3 to the L_2 XMCD intensity is largest for low coverages, characteristic of an increased orbital to spin magnetic moment ratio.

Figure 1(c) compares L_3 XMCD spectra normalized to the L_2 edge, for a cluster film with mass selection and two unfiltered depositions. The size range in the mass-selected

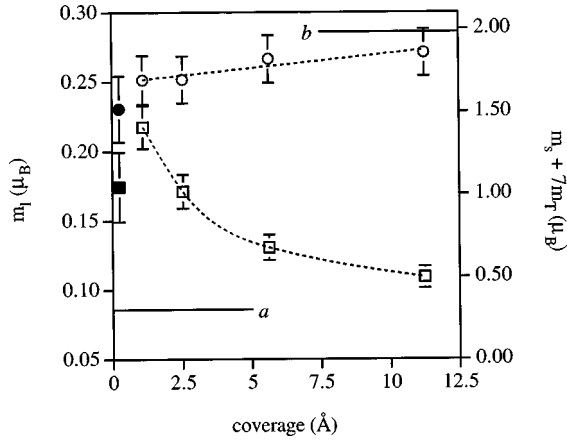


FIG. 2. Orbital (squares) and spin (circles) moments obtained for the Fe cluster films. The filled points at 0.25 Å coverage correspond to a mass-selected deposition. The dashed lines are to aid the eye. Lines marked *a* and *b* are the m_l and m_s obtained for a thick Fe film in Ref. 15.

film was restricted to 2.15 to 2.91 nm (441–1096 atoms) with a median diameter of 2.4 nm (610 atoms). The two unfiltered depositions show an identical line shape while that of the mass-filtered sample is clearly narrower which we ascribe to the reduced size range. Although this result does not reveal any magnetic information it is still important since it is independent evidence that there is some difference in the morphology of the cluster films between unfiltered and mass-filtered depositions.

Absolute values for m_l and m_s can be obtained by application of the XMCD sum rules. For the calculation of the intensity of $[I_{\uparrow\uparrow}(\omega) + I_{\downarrow\downarrow}(\omega)]$ an integral step function [shown in Fig. 1(a)] was fitted to the spectrum to remove the edge jumps. A value of 6.61 was used for the $3d$ occupation number n_h , as in Ref. 16. This is a reasonable choice although the clusters are likely to possess a modified band-structure compared to bulk Fe which affects the value of n_h . The white line intensity (proportional to n_h), however, is constant to within 5% with increasing coverage and so the uncertainty in n_h can only contribute a systematic error. An extra term $7m_T$, where $m_T = -\langle T_z \rangle \mu_B / h$, occurs in the spin sum rule, $\langle T_z \rangle$ being the expectation value of the magnetic dipole moment. Although this term is negligible for systems possessing cubic symmetry, it can become important at surfaces and interfaces,¹⁴ and so must be considered for the Fe cluster films.

Figure 2 shows how m_l and $(m_s + 7m_T)$ vary as a function of coverage in cluster films grown without mass selection. Also shown are transmission XMCD data for thick Fe films.¹⁶ The magnitude of m_l is very high at the lowest coverage and shows a significant variation as the density is increased. For the 1.1 Å film, the average cluster separation is ~ 12 nm so that the particles can be considered as isolated. In this sample the value of m_l is a factor of 2 larger than in the 11.3 Å film in which the average separation is ~ 2 nm and the clusters are touching. Clearly the cluster-cluster interactions cause a quenching of the orbital moment and we ascribe this to an increase in the average atomic coordination as clusters come into contact. It has been shown¹ that above a critical size, the clusters stay as separate entities and do not

coalesce into larger particles. We have confirmed this in a previous *in situ* STM study of Fe clusters on exposed and Ag terminated Si(111) surfaces in collaboration with the University of Nottingham.²² The images show that in dense films the clusters do not coalesce into fewer, larger entities. Rather, touching particles distort so that they have flat areas, containing a significant proportion of the surface atoms, in contact. A boundary line between them is, however, clearly visible so that they can be considered as strongly interacting but separate grains. Further evidence that the clusters do not form larger particles after landing is that the diameters of the deposited particles measured from the STM images (after correction for the tip radius) have the same size distribution as that measured in the free cluster beam by the mass filter.²² Although no images were taken for Fe clusters on HOPG there was no difference in the size distribution between the exposed and Ag terminated Si(111) surface and we assume it is also the same in the present system.

The value of $(m_s + 7m_T)$ for the unfiltered cluster depositions increases slightly with coverage. If this were due to the spin moment it would imply, contrary to all expectations for low coordination systems, that the spin moment was lowest in the isolated clusters. It is possible that the change is due to a variation in the number of valence band holes n_h but as stated earlier the total absorption cross section per atom (proportional to n_h) remains constant with coverage to within 5% while the spin+dipole term changes by 10%. Our favoured interpretation is that the increase in $(m_s + 7m_T)$ is due to a decrease in the dipole moment (opposite to the spin) with m_s remaining constant. We know from the previous STM study²² that in the unfiltered assemblies, 94% of the particles are larger than 500 atoms, in which the spin moment in free clusters^{4–7} has attained the bulk value. Thus even for the isolated clusters the data is expected to show the bulk m_s value. For the Fe(001) surface¹⁴ the dipole moment has a magnitude of about 10% of the spin moment so, if our interpretation is correct, the magnitude of the change seen in Fig. 2 would be produced by the dipole moment varying from the Fe(001) surface value to almost zero. Since the dipole moment is expected to be highest in low coordinated atoms, the change, as with the orbital moment, reflects the increasing proportion of clusters in contact thus increasing the average atomic coordination. Previous electron yield XMCD measurements from continuous Fe films^{12,13,25} have yielded values of the ratio $m_l / (m_s + 7m_T)$ comparable to the result reported here for the 11.3 Å cluster film.

For the mass-filtered samples, the filter window was set to the range 2.15–2.91 nm (441–1096 atoms). This wide setting was in order to deposit a measurable quantity of material in a short time to avoid contamination. The filtering function is a top hat so that the size distribution cuts off abruptly at the limits of 441 atoms and 1096 atoms. Within this range the most probable size is 2.3 nm (as in the unfiltered distribution) and the median size is 2.4 nm (610 atoms). Another important difference between the unfiltered and mass-filtered deposition is that in the latter case, the clusters are ionized and accelerated to about 20 eV (Ref. 19) whereas the unfiltered neutrals land with thermal energy. The free jet expansion in our source is too weak to significantly accelerate the clusters.

The measured values of m_l and $(m_s + 7m_T)$ for the mass-selected film are shown in Fig. 2. The orbital moment is smaller than in the lowest density unfiltered film which we ascribe to the absence of small clusters below 440 atoms. It is reasonable to assume that the enhancement in m_l over the bulk value is proportional to the fraction of surface atoms which increases approximately as the inverse of the cluster diameter in the size range studied here. Removing the smallest clusters will thus tend to lower the average value of m_l .

The $m_s + 7m_T$ term measured for the mass-selected film is around 15% *smaller* than the average value obtained for the unfiltered samples. The clusters in this film are sufficiently large that again, the spin moment will not be measurably larger than the bulk Fe (or the dense cluster film) value. It is possible that a decrease in the spin moment occurs as a result of a structural change in the particles, for example to the fcc or hcp phase induced by the higher impact energy. We rule this out however since if it occurred we would measure a significantly different XAS line shape compared to the unfiltered clusters rather than the slight narrowing observed. As in the case of the unfiltered films we ascribe the change in $m_s + 7m_T$ to be due to the dipole moment.

The changes in m_T and m_l when comparing low density mass-filtered and unfiltered depositions is in contrast to those observed for increasing density unfiltered films. In the latter case the variation in the orbital and dipole moments with coverage is due to the increasing average atomic coordination which decreases the value of both moments. In the mass-selected deposition we detect, relative to the lowest density unfiltered film an *increased* dipole moment and a *decreased* orbital moment. This detracts from the possibility that the changes are due to an increased mobility and coalescence of the mass-selected ions since in that case we would expect both moments to decrease as in the case of the higher density neutral depositions. We therefore ascribe this change to the increased impact energy producing extra distortion on landing which will increase the average asymmetry of the crystal field around the atoms without significantly affecting the average coordination. The result is an increase in the magnetic dipole term producing the low value of $m_s + 7m_T$ but not the orbital moment. This is a significant finding since it indicates that by varying the impact energy we can have independent control of attributes such as the dipole moment and particle anisotropy. This also demonstrates that XMCD is able to probe $\langle T_z \rangle$ with a high sensitivity in a system of randomly oriented particles. Methods which measure $\langle T_z \rangle$ directly would require that the clusters all had the same orientation with respect to the substrate.

Hysteresis curves can be measured using XMCD, by measuring the XAS intensity at the L_3 edge as a function of the applied field strength, at a fixed photon polarization. Out-of-plane hysteresis loops (i.e., measured with the sample surface normal to the photon beam) have a similar shape for all cluster films, with the magnetization saturating at ≈ 1 T and a coercivity of less than 0.1 T.

The ratio of remanence to saturation magnetization, measured in the out-of-plane direction, is shown in Fig. 3, for various cluster film densities. All unfiltered depositions studied during this experiment showed a small but measurable remanence, which increases per atom with coverage. The blocking temperature of isolated clusters with a diameter of

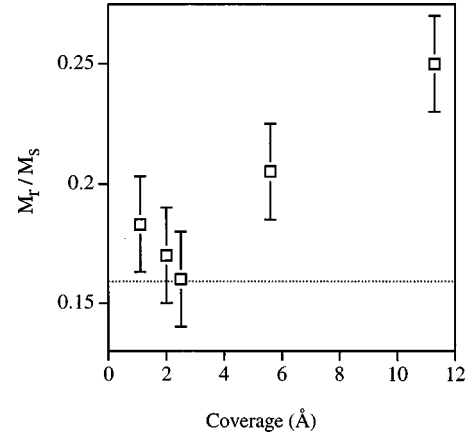


FIG. 3. Remanence to saturation magnetization ratio versus thickness of unfiltered Fe cluster films, measured using XMCD. Dotted line: M_r/M_s measured for a thick MBE film grown on HOPG.

2.3 nm is 1 K assuming the bulk Fe anisotropy constant ($4.5 \times 10^4 \text{ J m}^{-3}$) or 8 K using the published value for nanoscale Fe grains in Al_2O_3 (10^6 J m^{-3}).²⁶ If all the particles were this size and were noninteracting, therefore, we would not expect to measure a remanent magnetization at 10 K. We believe the remanence arises from the fact that there is a size distribution and as the coverage is increased the larger clusters, which are below their blocking temperature, will interact with and magnetize (by the exchange interaction) smaller clusters which, if isolated, would be above their blocking temperature. An alternative explanation is that the perpendicular remanent magnetization is due to the roughness-related anisotropy of the cluster-generated film. A previous magnetic linear dichroism experiment²⁷ which measured the in-plane remanence as a function of cluster coverage showed the same trend as in Fig. 3. The result is therefore independent of the magnetization direction and we rule out the alternative model.

In conclusion we have demonstrated that isolated nanoscale Fe clusters, either size-selected (2.4 nm) or with a log-normal size distribution peaking at 2.3 nm, supported on HOPG have an orbital magnetic moment m_l a factor of two greater than the bulk value. This decreases with cluster density on the surface and converges to the bulk value when the clusters are in contact. The measured spin moment m_s for the unfiltered clusters is, to within experimental error, independent of coverage. We thus attribute the increased value of m_l to a less effective quenching by the crystal field due to the reduced average atomic coordination. The mass-filtered film shows a lower value of $m_s + 7m_T$ than the unfiltered depositions which we ascribe to an increase in the magnetic dipole moment due to the higher energy of the ions producing a greater distortion on impact with the surface. The cluster films exhibit remanence which increases with cluster density and is a result of larger clusters below their blocking temperature interacting with and magnetising smaller clusters which if isolated would be above their blocking temperature.

We gratefully acknowledge EPSRC support on Grant No. GR L 88931 for the transport of the cluster source to Grenoble and the expert technical assistance provided by Kenneth Larsson during the experiment.

- ¹P. Melinon, V. Paillard, V. Dupuis, A. Perez, P. Jensen, A. Hoareau, J. P. Perez, J. Tuailon, M. Broyer, J. L. Vialle, M. Pellarin, B. Baguenard, and J. Lerme, *Int. J. Mod. Phys. B* **9**, 339 (1995).
- ²R. Kubo, *J. Phys. Soc. Jpn.* **17**, 975 (1962).
- ³C. Binns, C. Norris, H. S. Derbyshire, and C. Norris, in *Physics and Chemistry of Finite Systems: from Clusters to Crystals*, edited by P. Jenna, S. N. Khanna, and B. K. Rao (Kluwer, Dordrecht, 1992).
- ⁴J. P. Bucher, D. C. Douglass, and L. A. Bloomfield, *Phys. Rev. Lett.* **66**, 3052 (1991).
- ⁵I. M. L. Billas, A. Châtelain, and W. A. De Heer, *Science* **265**, 1682 (1994).
- ⁶I. M. L. Billas, W. A. De Heer, and A. Châtelain, *J. Non-Cryst. Solids* **179**, 316 (1994).
- ⁷I. M. L. Billas, J. A. Becker, A. Châtelain, and W. A. de Heer, *Phys. Rev. Lett.* **71**, 4067 (1993).
- ⁸A. J. Cox, J. G. Louderback, S. E. Apsel, and L. A. Bloomfield, *Phys. Rev. B* **49**, 12 295 (1994).
- ⁹G. M. Pastor, J. Dorantes-Dávila, S. Pick, and H. Dreyssé, *Phys. Rev. Lett.* **75**, 326 (1995).
- ¹⁰J. P. Chen, C. M. Sorensen, K. J. Klabunde, and G. C. Hadjipanayis, *Phys. Rev. B* **51**, 11 527 (1995).
- ¹¹D. M. Duffy and J. A. Blackmann (unpublished).
- ¹²B. T. Thole, P. Carra, F. Sette, and G. van der Laan, *Phys. Rev. Lett.* **68**, 1943 (1992).
- ¹³P. Carra, B. T. Thole, M. Altarelli, and X. Wang, *Phys. Rev. Lett.* **70**, 694 (1993).
- ¹⁴R. Wu and A. J. Freeman, *Phys. Rev. Lett.* **73**, 1994 (1994).
- ¹⁵F. M. F. deGroot, *J. Electron Spectrosc. Relat. Phenom.* **67**, 529 (1994).
- ¹⁶C. T. Chen, Y. U. Idzerda, H.-J. Lin, N. V. Smith, G. Meigs, E. Chaban, G. H. Ho, E. Pellegrin, and F. Sette, *Phys. Rev. Lett.* **75**, 152 (1995).
- ¹⁷W. L. O'Brien and B. P. Tonner, *Phys. Rev. B* **50**, 12 672 (1994).
- ¹⁸M. Drescher, G. Snell, U. Kleineberg, H.-J. Stock, N. Müller, U. Heinzmann, and N. B. Brookes, *Rev. Sci. Instrum.* **68**, 1939 (1997).
- ¹⁹S. H. Baker, K. W. Edmonds, A. M. Keen, S. C. Thornton, C. Norris, and C. Binns (unpublished).
- ²⁰S. H. Baker, S. C. Thornton, A. M. Keen, T. I. Preston, C. Norris, K. W. Edmonds, and C. Binns, *Rev. Sci. Instrum.* **68**, 1853 (1997).
- ²¹M. D. Upward, P. Moriarty, P. H. Beton, S. H. Baker, C. Binns, and K. W. Edmonds, *Appl. Phys. Lett.* **70**, 2114 (1997).
- ²²M. D. Upward, Ph.D. thesis, University of Nottingham, 1998.
- ²³J. Stöhr and R. Nakajima, *J. Phys. IV* **7**, 47 (1997).
- ²⁴H. Durr, G. van der Laan, D. Spanke, F. U. Hillebrecht, and N. B. Brookes, *Phys. Rev. B* **56**, 8156 (1997).
- ²⁵J. Stöhr and H. König, *Phys. Rev. Lett.* **75**, 3748 (1995).
- ²⁶C. L. Chien, in *Science and Technology on Nanostructured Magnetic Materials*, edited by G. C. Hadjipanayis and G. A. Prinz (Plenum, New York, 1991).
- ²⁷K. W. Edmonds, C. Binns, S. H. Baker, S. C. Thornton, and A. M. Keen (unpublished).